

Review of Impact and Solidification of Molten Thermal Spray Droplets

R.C. Dykhuizen

The unique properties of coatings created by thermal spray deposition depend on the rapid solidification of individual splats created by impinging molten droplets. However, the impact process has been little studied because of the difficulty of measuring or numerically simulating the process, which occurs very quickly over a small area. Other scientific fields have investigated the impact of liquid droplets on solid surfaces. This paper reviews these studies, along with those conducted specifically on the thermal spray process. Modelers have almost universally ignored droplet solidification during impact; however, some experimental evidence suggests that the solidification process plays a significant role in splat formation. Splashing of impacting liquid droplets, another topic that has been largely ignored, affects deposition efficiency, porosity, and bond strength, and may also affect the amount of oxides incorporated in the coating. The scaling of data from impacting millimeter-size droplets traveling at low velocities to thermal spray conditions is questioned.

1. Introduction

COATINGS produced by thermal spray deposition are used to enhance the wear, or corrosion, or thermal capabilities of a surface, or to rebuild worn or damaged surfaces. The unique properties of such coatings depend on the rapid solidification of individual splats created by impinging molten droplets. However, the impact process has been little studied because of the difficulty of measuring or numerically simulating the process, which occurs very quickly over a small area.

The object of this review is to determine those parameters (i.e., impact velocity, liquid viscosity, liquid superheat) that control splat size and solidification rate. These quantities directly influence coating properties. Droplet splashing also is of interest because it affects deposition efficiency, porosity, and bond strength. Splashing may also affect the amount of oxides that are incorporated into the coating; small splashed particles may oxidize quickly and can be driven back onto the surface by the gas flow field associated with thermal spraying. The impact of liquid droplets on solid surfaces is important in studying the erosion of aircraft surfaces caused by flight through clouds and rainstorms, the erosion of turbine blades operating in wet steam, and the erosion of terrestrial surfaces during rain. A limited number of studies have considered liquid impact during ink-jet printing and in the production of fine powders via impact atomization. This paper reviews experimental and analytical studies of the impact phenomenon for various applications to determine which aspects can be applied to the thermal spray process.

A few review articles have focused specifically on the thermal spray process. However, the impact and solidification process has not been considered in detail. Apelian et al. (Ref 1) concentrated on plasma spray particle heating rates during

Keywords: droplet solidification, impact modeling, Madejski model, review, splashing

R.C. Dykhuizen, Thermal and Fluid Engineering Department, Sandia National Laboratories, Albuquerque, NM 87185, USA

Nomenclature	
c	speed of sound (m/s)
C	thermal heat capacitance (J/kg · K)
d	droplet diameter (m)
D	splat diameter (m)
h	splat thickness (m)
K	thermal conductivity (W/m · K)
L	heat of solidification (J/kg)
Pe	Peclet number, ud/α_S
Q	heat flux (W/m ²)
\mathcal{R}	contact resistance (K · m ² /W)
Re	Reynolds number, $\rho_L u d/\mu$
t	time measured from impact (s)
T	splat cooling rate (K/s)
T	temperature (K)
U	dimensionless velocity parameter
u	droplet impact velocity (m/s)
We	Weber number, $\rho_L u^2 d/\sigma$
y	contact ring location (m)
Greek	
α	thermal diffusivity (m ² /s)
δ	thickness of solid layer (m)
ξ	flattening parameter, D/d
σ	surface tension (J/m ²)
ρ	density (kg/m ³)
θ	nondimensional temperature
μ	droplet viscosity (N · s/m ²)
ϕ	angle depicted in Fig. 2
Subscripts	
b	substrate
bo	initial substrate
L	liquid
melt	melting point
N	nucleation
po	initial particle
S	solid

flight and cooling rates after impact. The flow during impact was only briefly considered. Zaat (Ref 2) and Fisher (Ref 3) reviewed plasma spraying from arc heating to droplet solidification. However, they only briefly considered the impact process and provided no references for this subtopic. Safai and Herman (Ref 4) provided another general review of plasma spraying, concentrating on the properties and grain structure of the coatings produced. The authors did state that the splat size is smaller for rough surfaces, and this was later verified by Fantassi et al. (Ref 5). Mash et al. (Ref 6) devoted a large portion of their review of plasma spraying to the relationship between deposition efficiency and process parameters.

Experimental data on the flattening of thermal spray droplets are scarce due to the difficulty of obtaining accurate data on the thermal and kinetic energy of the micrometer-size droplets prior to impact. Experimental data are available for the flattening ratio as a function of thermophysical properties for millimeter-size drops traveling at low velocities. These millimeter experiments are conducted so that nondimensional parameters defined by the experimenters are the same as those found in thermal spray processes. However, it is shown here that the scaling of these results over three orders of magnitude in physical size may not be possible. Finite nucleation times and contact resistances, which are of no consequence in the millimeter-size experiments, become important in the thermal spray processes.

A number of analytical studies have investigated the flow of liquid droplets during impact on a solid surface. Most do not consider the solidification of the droplet. Experimental evidence suggests that partial solidification upon impact influences the flow of the molten droplet.

2. Experimental Observations of Impact and Solidification

Several papers offer experimental observations that relate to the impact and solidification of droplets on a substrate. A number of papers have investigated the impact of raindrops (Ref 7-10). Two interesting conclusions are often stated in this body of literature. First, the liquid that makes up the portion of the drop that first impacts the surface ends up at the periphery of the splat. Second, drops impacting on smooth, dry surfaces do not splash. Splashing will occur if the surface is rough or wet.

Models of thermal spray droplet impacts do not include splashing, even though the substrate is never smooth (especially after the initial layer of splats has formed). It is experimentally found from the raindrop studies that the number of secondary splash drops increases with increasing impact velocity, drop size, and surface roughness. This seems to indicate a Reynolds number dependence. Surface tension caused only a weak dependence on the number of secondary drops (Ref 8, 11). Since water drops often do not wet the solid surface, much has been published on the oscillation of the sessile drops (Ref 12-14). None of these raindrop studies considered solidification, but instead emphasized erosion.

Some raindrop studies investigated impacts on surfaces that were not flat or impact angles that were not normal (Ref 9, 14,

15). These studies could possibly be used to help verify a numerical simulation. Shi and Dear (Ref 15) reported that the radial spreading velocity of a liquid impacting a solid surface is approximately three times the impact velocity.

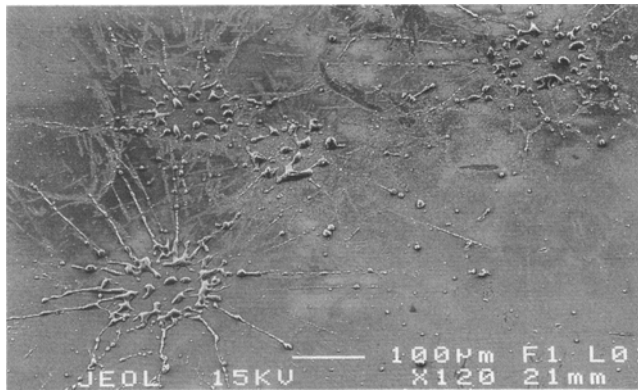
Early experimental work applied to the impact of water droplets on turbine blades was presented by Savic and Boulton (Ref 16), who showed that a normal impact onto a smooth surface produces no splashing. Experimental pictures of the impact of hot wax onto a cold surface revealed significant splashing. The authors claimed that this was due to the solidification of the lowest part of the drop as it flowed out radially; portions of the drop were ejected upward as it flowed over the solidified portion. This concept is consistent with observations by Engel (Ref 10), who showed that the lowest portion of the drop flows out to the periphery of the splat. This portion may solidify first since it is the first to contact the cold substrate, and then moves outward in contact with more unheated substrate.

Droplet impact is also important in the study of ink-jet printing (Ref 17) and impact atomization processes for powder production (Ref 18-20). However, these studies did not reveal any information applicable to thermal spraying that was not already obtained from the water impact studies cited earlier.

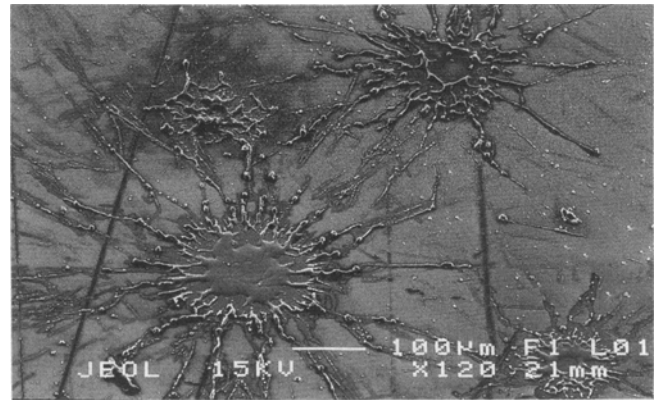
Droplet impact studies conducted to investigate thermal spray applications are demanding due to the difficulty of measuring the droplet velocity, size, and molten condition just prior to impact. Also, property evaluation for many high-temperature plasma-sprayed materials is complicated. Therefore, many experimenters use large drops (on the order of millimeters) and well-characterized materials (Ref 21-23). These millimeter experiments are conducted so that the nondimensional parameters as defined by the experimenters are the same as those found in thermal spray processes. However, as is later shown in this paper, all of the processes that control the solidification rate are not included in the models presented, and other nondimensional parameters are not identical. Therefore, the millimeter experimental results cannot be applied to thermal spray conditions.

Some experiments considered the thermal spray processes directly. Moore et al. (Ref 24) observed that thermal-sprayed droplets resulted in more breakup upon impact at higher velocities. Breakup is inferred by examining the solidified splat; data on the splash products (splash size, angle of rebound, etc.) are not available. These data, along with those of Savic and Boulton (Ref 16), offer the only indication of splashing of a drop on a smooth, dry surface—in direct contrast to the water droplet studies, which did not consider solidification. Moore et al. (Ref 24) observed that deposition efficiency improved when the substrate was heated. This may indicate less splashing at a higher substrate temperature due to a lower solidification rate. This agrees with the observation of Savic and Boulton (Ref 16) that an increased droplet superheat reduces splashing.

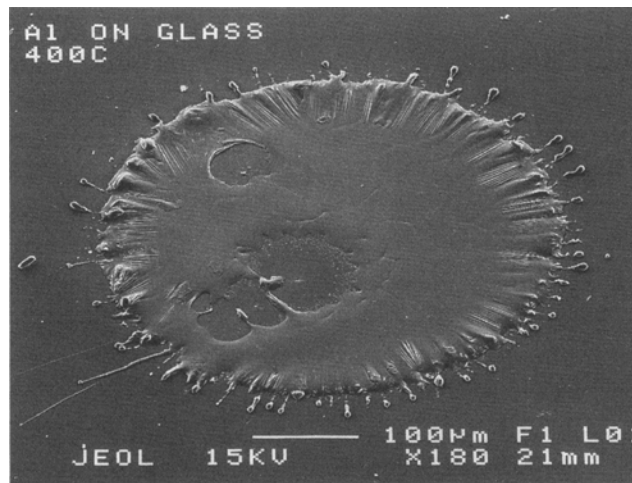
Hasui et al. (Ref 25) showed that alumina splat shapes are greatly influenced by substrate temperature. Experiments conducted with smooth substrates showed that regularly shaped disks were created for high substrate temperatures and that star-shaped patterns were created for low substrate temperatures. Hasui et al. stated that the star shapes result from splashing upon impact. However, Houben (Ref 26) demonstrated splashing from both disk and star splat shapes. A possible explanation for splashing upon impact onto a smooth substrate is that given by



(a)



(b)



(c)

Fig. 1 Variations in aluminum splat geometries as a function of the smooth glass substrate temperature. Note how a progression from a star-shaped splat to a regularly shaped disk is obtained as the substrate temperature is increased. Substrate temperature: (a) 20 °C; (b) 200 °C; (c) 400 °C

Savic and Boulton (Ref 16). However, variations with temperature in the wetting of the droplet on the substrate could also influence the final splat shape in a similar manner (Fig. 1a) (Ref 27).

The Hasui et al. (Ref 25) experiment was repeated at Sandia National Laboratories using different metal droplets impacting on metal and glass substrates. In all cases, the substrate temperature greatly influenced splat geometry. Figure 1 shows how aluminum splat shapes varied with glass substrate temperature. A progression from a star-shaped splat obtained at low temperatures to a regularly shaped disk at 400 °C is evident. Star-shaped splats were always obtained on rough glass substrates regardless of substrate temperature (Ref 28).

Predecki et al. (Ref 29) observed splat cooling rates deposited on an inclined substrate. However, they did not report on the splat geometries found in sufficient detail to determine the flow of the molten material prior to solidification.

Many papers have investigated and presented photographs of individual thermal spray droplet splats (Ref 21, 24-26, 30-34). These studies showed that disk shapes are not always produced. Kudinov et al. (Ref 30) discussed how different splats may appear, depending on the fraction of the droplet

that is not molten. Estimates of size, velocity, and heat content of the droplet before impact were not available until recent experiments by Fantassi et al. (Ref 5, 35). Here, the intensity of two-color infrared detectors was used to determine droplet size, splat size, and temperature histories. The time delay between signals also yielded velocity information. The results were only approximate because the model used to reduce the data implicitly assumed that the entire splat surface was at a uniform, although time varying, temperature during the transient. The material was also assumed to behave as a gray emissive body and the splats were disk shaped. The experimental data exhibited much scatter. It is unclear whether the scatter arose from errors in collecting the experimental quantities or from errors in the assumptions, or whether the flattening ratio (splat diameter over initial droplet diameter) is a function of other parameters not measured or controlled. Fantassi et al. (Ref 35) showed that surface roughness affects the resulting flattening of the droplet. Madejski (Ref 21) and Hasui et al. (Ref 25) showed that the angle of impact of droplets can affect splat geometry and coating properties. These observations have yet to be incorporated into any model of droplet impact.

3. Impact Models

Numerous two-dimensional models have been presented that analyze the impact of a nonsolidifying liquid droplet on a smooth plane. These models consider either a spherical droplet or a cylindrical droplet (with the axis of the cylinder parallel to the impact plane). An axisymmetric assumption, used in the spherical droplet models, limits the investigation to an initial droplet velocity normal to a flat surface, or onto an axisymmetric surface. The use of a cylindrical droplet allows use of geometries that can be represented in two-dimensional Cartesian coordinates; however, extension of these results to the actual spherical drop is difficult. Instabilities that may yield breakup upon impact (e.g., the classical crown splash geometries in Ref 27) cannot be resolved in any two-dimensional model. This section discusses incompressible and compressible models. The compressible models resolve very early time periods when the compression wave generated by the impact has not yet traveled throughout the droplet. Studies that consider solidification are reviewed in the next section.

3.1 Incompressible Models

Incompressible models of the impact process offer a simplified examination of the radial flow of the liquid droplet during impact. A simple scaling argument shows that the results from this model cannot be correct for early times on the order of:

$$t_c \approx \frac{d}{c} \quad (\text{Eq 1})$$

where c is the speed of sound (m/s) in the liquid. Trapaga and Szekely (Ref 36) have shown that the time scale of the impact process can be given as:

$$t_1 = \frac{2d}{3u} \text{Re}^{0.2} \quad (\text{Eq 2})$$

This is found to be at least an order of magnitude longer than the compressible flow time (t_c), and thus an incompressible assumption should yield reasonable results. Peak pressures at early times will, of course, not be resolved.

Savic and Boulton (Ref 16) made an early analytical study of spherical droplets impacting onto a solid surface. They posed the problem as one of potential flow in an approximate geometry. Their predicted drop spreading during the early portion of low-velocity impacts agreed fairly well with their experimental data.

Harlow and Shannon (Ref 37) presented numerical calculations of a spherical drop impacting upon a flat surface. Impact into a liquid pool was also considered, however, these calculations are of no concern to thermal spraying because the previous droplets are solidified before new molten droplets impact the substrate. Harlow and Shannon (Ref 37) neglected surface tension, viscosity, and compressibility. Their two-dimensional (axisymmetric) calculations showed that the liquid film created travels radially at 1.6 times the drop initial velocity (independent of all other parameters). No splashing was resolved. Limited data comparisons at early times were good. However, because all the mechanisms that would limit the growth of the

splat were ignored, the numerical simulation did not yield a final splat diameter.

Trapaga and Szekely (Ref 36) presented an improved model of droplet impingement. Their model is similar to that of Harlow and Shannon (Ref 37) except that viscosity and surface tension are included. They predicted that the liquid film radial velocity is about three times the initial drop velocity (which agrees with the experimental data of Shi and Dear [Ref 15]). The final droplet size is not sensitive to the liquid surface tension for parameters representing plasma spray applications. This is especially true for cases where the liquid wets the substrate (wetting was simulated with a contact angle of 10°). Trapaga and Szekely (Ref 36) reported breakup of the splat for a nonwetting liquid; however, their results were not independent of the mesh size used. Their results have the same trends as found numerically by Madejski (Ref 21), but show a slightly smaller splat diameter. Watanabe et al. (Ref 38) provided an analysis using very similar techniques and obtained results very similar to those of Trapaga and Szekely (Ref 36).

Liu et al. (Ref 39) presented numerical calculations of a spherical droplet impacting upon a flat surface. Their model assumptions were similar to those of Trapaga and Szekely (Ref 36). They predicted that the liquid film travels radially at twice the droplet initial velocity. No splashing was resolved. Limited data comparisons at early times were good. However, the calculations were not carried out long enough to show the final (or maximum) splat size as was done by Trapaga and Szekely (Ref 36).

3.2 Compressible Models

Due to their complexity, compressible models have only been used to study the initial impact of a droplet upon a solid substrate. Results on final splat sizes have not been obtained.

Engel (Ref 10) identified the need for compressible modeling to obtain the peak pressures during droplet impact. She was the first to identify all of the physics associated with a compressible sphere of fluid impinging upon a planar surface. As shown in Fig. 2, the undisturbed fluid continues at a downward velocity of u . The contact ring location, y , can be expressed as a function of the angle defined in Fig. 2:

$$y = \frac{d}{2} \sin \phi \quad (\text{Eq 3})$$

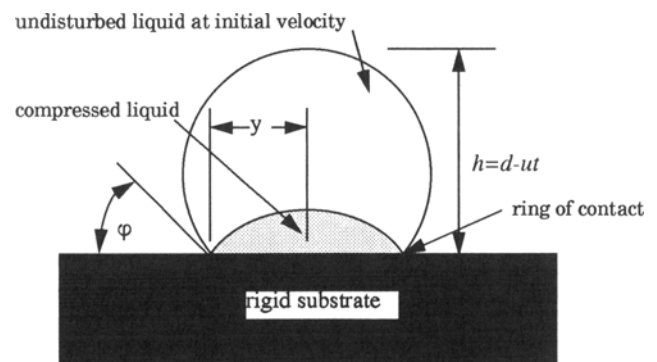


Fig. 2 Subcritical flow regime during liquid droplet impact onto a solid substrate

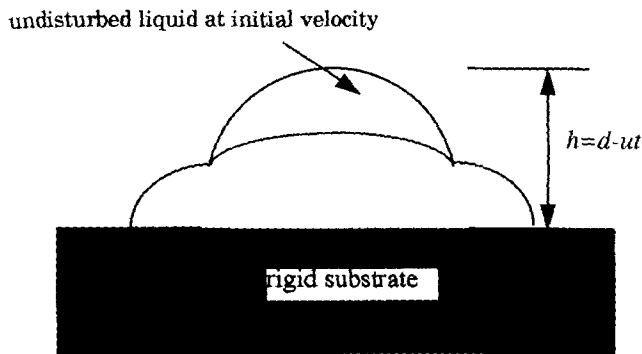


Fig. 3 Postcritical flow regime during liquid droplet impact onto a solid substrate

When Eq 3 is differentiated with respect to time, the outward velocity of the contact ring can be determined. As long as this ring velocity is greater than the sonic speed in the liquid droplet, the shock wave separating the compressed liquid from the undisturbed liquid will be attached to the contact ring and the shape of the droplet is a truncated sphere (as shown in Fig. 2). Thus, Eq 4 can be used to determine at what angle ϕ this flow period ends and radial spreading of the liquid droplet can start. Later authors identified this initial period as the subcritical flow period.

$$c = \frac{dy}{dt} = \frac{u}{\tan \phi} \quad (\text{Eq 4})$$

Heymann (Ref 40) presented an analysis of the compressible stage of the impact of a liquid droplet and showed that the maximum impact pressure of a spherical droplet is larger than the classical water hammer pressure (ρcu). This fact was later confirmed experimentally by Rochester and Brunton (Ref 41) and is due to the spherical geometry of the droplet. The contact area between the droplet and the substrate in the subcritical regime can be calculated from the initial droplet shape and the initial droplet velocity (see Fig. 2). The postcritical flow stage (Fig. 3) results in radial spreading of the droplet driven by the high pressures in the compressed liquid. Heymann's analysis assumes that the axisymmetric droplet can be represented by a two-dimensional Cartesian cylinder of liquid, the cross section of which is shown in Fig. 2. Heymann (Ref 40) and Trapaga and Szekely (Ref 36) discuss how the assumption of a cylindrical droplet (with its axis parallel to the substrate) may be extended to the actual case of spherical droplets.

Huang et al. (Ref 42) presented numerical results for the impact of a spherical droplet on a rigid plane. Their results spanned both subcritical and postcritical flow. Since the model ignores viscosity and surface tension, final splat diameters were not obtained. The results are not likely to be very accurate due to the approximations involved in the finite differences used. The pressures reported were less than those obtained by Heymann (Ref 40).

At the Sixth International Conference on Erosion by Liquid and Solid Impact, a series of papers discussed the compressible flow during impact of a liquid droplet on a flat surface (Ref 43-45). The initial jet of liquid, after the shock wave detaches from the substrate, is directed toward the substrate. There is some evi-

dence that this liquid may rebound from the substrate and create a mist. It is unclear how much of this is applicable to thermal spray droplets since the rebounding spray will likely be intercepted by the downward flowing drops when the ratio of the droplet impact velocity to the speed of sound in the liquid is so low.

4. Phenomenological Impact Models for Thermal Spray Applications

A few models have been developed for analyzing droplet impact for thermal spray applications. Some of these models are quite complex and require computer solutions. However, phenomenological models have been proposed to describe the impact and solidification process. These models do not attempt to capture the entire process in detail, but rather to determine the proper dimensionless parameters that describe the process. All the models assume a normal impact upon a smooth substrate.

Jones (Ref 46) provided one of the earliest models for determining the flattening ratio of a liquid drop impinging upon a solid substrate. He ignored surface tension and solidification effects based on the results of a scaling analysis. His result for final splat size is as follows:

$$\xi = 1.16 (\text{Re})^{0.125} \quad (\text{Eq 5})$$

Most recent authors prefer the later work by Madejski (Ref 21). Madejski does not consider compressibility of the liquid, but does include surface tension, viscosity, and solidification. His result is splat size as a function of three dimensionless parameters that determine the relative importance of these three processes. The Reynolds number (Re) is used to scale the viscous dissipation of the inertial forces, the Weber number (We) is used to scale transformation of the kinetic energy to surface energy, and a modified Peclet number (Pe) is used to scale solidification rates.

Madejski's full model includes all three of these dimensionless numbers and results in a complex integral-differential equation that does not have an analytic solution. Therefore, Madejski presents results in the form of numerical fits. For example, his most quoted result is for the case where the dominant mechanism during impact is the decay of kinetic energy via viscous dissipation. This is referred to in this paper as the Madejski flow model:

$$\xi = 1.2941 (\text{Re} + 0.9517)^{0.2} \quad (\text{Eq 6})$$

Fiedler and Naber (Ref 47) presented an analysis very similar to that derived by Madejski, except that the solidification process is not included. Their result is almost identical. They also showed that the splat diameter for large Weber numbers is dependent only on the Reynolds number.

Trapaga and Szekely (Ref 36) provided a fit to their numerical results of droplet flow after impact. This yields a similar form, but a smaller coefficient:

$$\xi \approx 1.0 (\text{Re})^{0.2} \quad (\text{Eq 7})$$

A second mechanism that can limit the growth of a splat is the conversion of kinetic energy to surface energy. When this

mechanism dominates, Madejski presents the following fit to his numerical results, which is limited to large Weber values (but which are still sufficiently small so that solidification and viscous effects are negligible):

$$\xi = \sqrt{\frac{We}{3}} \quad (\text{Eq 8})$$

Using Madejski's differential equations for this case, it is possible to obtain an analytical expression that is not limited to large values of the Weber number:

$$We = 3\xi^2 + \frac{8}{\xi} - 11 \quad (\text{Eq 9})$$

However, the modeling assumptions proposed by Madejski for surface energy are questionable. Madejski ignores the surface energy associated with the liquid/solid and gas/solid interfaces, and considers only the liquid/gas interface. This results in a model that is independent of the liquid contact angle. The dependence of droplet motion on the contact angle for low Weber number flows is well known (Ref 48). Therefore, Madejski's result is valid only for the special case of a 90° contact angle, where the two ignored surface energies will cancel.

From a different model, Cheng (Ref 13) investigated the growth of a nonsolidifying splat that does not wet the substrate. He derived a significantly different expression for the maximum size when surface tension is the only retarding force to splat growth:

$$\xi = 0.816 (We)^{0.25} \quad (\text{Eq 10})$$

From scaling analysis (Ref 21, 46, 47), the surface tension forces are shown to be unimportant to the thermal spray application. Therefore, surface tension will not be considered further in this review.

Madejski's third mechanism concerns the solidification of the splat. The formulation of this model in Madejski's paper is very complex. The solidification model can be derived in a more approximate manner that allows easier interpretation of the result. First consider that the thickness of the splat can be determined from the time since impact via Eq 11, which assumes that the trailing end of the droplet continues at the initial velocity toward the substrate (see Fig. 2 and 3):

$$h = d - ut \quad (\text{Eq 11})$$

Madejski's model calculated a solidified thickness that varied as a function of radial position in the splat. This variation, although real, will be ignored here. Equation 12 determines the single solidified layer thickness in the present simplified model. As was done by Madejski, a nondimensional constant, U, is introduced to determine the conduction-limited growth of the solidified layer. Its value will be determined later and will be on the order of unity:

$$h = U\sqrt{\alpha_S t} \quad (\text{Eq 12})$$

where α_S is the thermal diffusivity of the solidified layer. By setting Eq 11 and 12 equal, the time that the solidified layer equals the splat thickness (and thus flow stops) can be deter-

mined. Using this time, the final thickness of the solidified splat can be obtained:

$$h = \frac{U^2 \alpha_S}{2u} \left(\sqrt{1 + \frac{4du}{\alpha_S U^2}} - 1 \right) \quad (\text{Eq 13})$$

By assuming that the following group

$$\frac{4du}{\alpha_S U^2} \quad (\text{Eq 14})$$

is large compared to unity, the solution becomes:

$$\frac{h}{d} = U \sqrt{\frac{\alpha_S}{ud}} = \frac{U}{\sqrt{Pe}} \quad (\text{Eq 15})$$

Next, using the following identity (assuming a disk-shaped splat of diameter D),

$$\frac{h}{d} = \frac{2}{3} \left(\frac{d}{D} \right)^2 \quad (\text{Eq 16})$$

the flattening parameter is estimated:

$$\xi = 0.82 \left[\frac{Pe}{U^2} \right]^{0.25} \quad (\text{Eq 17})$$

Equation 17 compares well with what was numerically determined by Madejski from a much more complex model:

$$\xi = 1.49 \left(\frac{\rho_L}{\rho_S} \right)^{0.395} \left[\frac{Pe}{U^2} \right]^{0.1975} \quad (\text{Eq 18})$$

The dimensionless constant U remains to be determined. Madejski first tried to use the constant as derived from the Stefan problem (Ref 49):

$$\begin{aligned} & \frac{K_b \sqrt{\alpha_S} e^{-(U/2)^2}}{K_S \sqrt{\alpha_b} + K_b \sqrt{\alpha_S} \operatorname{erf}(U/2)} \\ & - \frac{K_L \sqrt{\alpha_S} (T_{po} - T_{melt}) e^{-\alpha_S U^2 / 4 \alpha_L}}{K_S (T_{melt} - T_{bo}) \sqrt{\alpha_L} \operatorname{erfc}(U \sqrt{\alpha_S / \alpha_L} / 2)} \\ & = \frac{UL\sqrt{\pi}}{2C_S(T_{melt} - T_{bo})} \quad (\text{Eq 19}) \end{aligned}$$

Equation 19 determines the dimensionless constant U for the one-dimensional case of a molten layer at initial temperature T_{po} , that comes in contact with a substrate at initial temperature T_{bo} .

Madejski determined that the use of Eq 19 resulted in the flattening of the splat becoming a function of the substrate thermal properties, which was in direct conflict with his data. Therefore, it was assumed that the substrate remained isothermal during the cooling process, a phenomenon for which two explanations are possible. One might be that the heat was drawn out of the substrate from an area much larger than the splat interface. There-

fore, the one-dimensional assumption in the Stefan problem was incorrect. A multidimensional conduction solution would make the interface closer to isothermal. Another possible explanation is that the largest thermal resistance retarding heat removal from the splat is a contact resistance between the splat and substrate (the Madejski model does not include a contact resistance). If this resistance does not vary much with the substrate material, a model that does not depend on substrate properties is more correct. Either physical explanation would result in the heat-transfer rate being less dependent on the properties of the substrate, but not as high as the heat-transfer rate calculated by Madejski from the isothermal assumption.

The isothermal assumption required that the constant U be found from Eq 20 (which can be obtained in the limit of infinite conductivity of the substrate in Eq 19):

$$\frac{C_S(T_{\text{melt}} - T_{\text{bo}})}{L} = \sqrt{\pi} \left(\frac{U}{2} \right) \operatorname{erf} \left(\frac{U}{2} \right) e^{(U/2)^2} \quad (\text{Eq 20})$$

Madejski concluded that the solidification mechanism was the controlling parameter. He had low-speed data from molten lead impacts and high-speed data from plasma spray alumina impacts. However, he stated that "the accuracy of the experiments left much to be desired...."

5. Applications of the Thermal Spray Phenomenological Models

5.1 Madejski Model

For most thermal spray applications, the Madejski solidification model results in a smaller splat than use of the flow (viscous dissipation) and surface tension models proposed by Madejski. One might therefore conclude that the solidification process is the dominant mechanism in limiting growth of the splat. However, most investigators have ignored Madejski's suggestion that the solidification model is dominant. This is typically based on estimates of solidification times from experimental data. Also, the fact that Madejski was forced to give up the Stefan model (Eq 19) for determination of the solidification parameter made some investigators less confident of the solidification model (Ref 1).

Which process is dominant in determining the splat size for a particular thermal spray application: flow or solidification? Both mechanisms have a velocity dependence to the 0.2 power (Eq 6 and 18); thus, this parameter alone does not distinguish which mechanism is controlling. The other terms in the correlation must be considered.

Property evaluation for these mechanisms is difficult. Many properties are not available (e.g., the viscosity of molten tungsten, the thermal conductivity of molten titanium). Other properties vary significantly between the substrate and melting temperature (e.g., the thermal conductivity of solid zirconia), and the model assumes a constant value.

For tests that use large, millimeter-size drops and well-characterized materials (e.g., lead), application of the Madejski model determines that the solidification mechanism is controlling. Final splat sizes predicted when only solidification is considered are smaller than when only viscous dissipation is

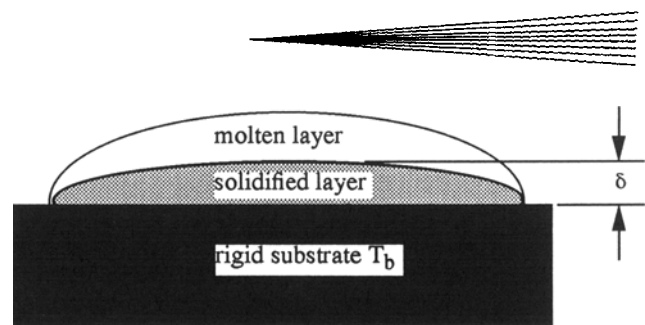


Fig. 4 Heat path from substrate to solid-liquid interface

considered. Therefore, solidification will limit the growth of the splat. The millimeter data (Ref 21, 22) are well represented by the Madejski solidification model (Eq 18).

The thermal spray experiments, with small particles and large velocities, result in magnitudes for the three nondimensional parameters proposed by Madejski that are similar to those obtained by the millimeter droplet experiments. Therefore, the Madejski models again predict that the solidification process acts faster than the viscous dissipation process. However, one might question how well the model applies to the thermal spray case. If the impact time is scaled by the droplet diameter divided by the droplet velocity (as implied by Eq 12 and 15 for the solidification process, and derived by Trapaga and Szekely [Ref 36] for the flow dissipation process), then the millimeter experiments have an impact time of 0.3 ms. This can be compared to a typical impact time of 0.1 μ s for thermal spray applications. The three-orders-of-magnitude difference raises questions about the similarity of the two experiment sets despite their similar nondimensional parameters. It is felt that the three nondimensional parameters proposed by Madejski do not completely describe the relevant processes. The following section discusses how the splat flattening process varies from the Madejski model.

5.2 Contact Resistance and Nucleation Delays

The scaling argument by Jones (Ref 46) is often quoted to dismiss the solidification mechanism in favor of viscous dissipation for thermal spray conditions. Jones predicts that the solidification is significantly slower than later predicted by the Madejski model due to a thermal contact resistance between the splat and the substrate. In fact, Jones determines that the solidification process is so slow that it need not be considered when determining final splat sizes. The Madejski model ignores any contact resistance and thus reaches a different conclusion. That a significant thermal contact resistance exists has been proved experimentally. Safai and Herman (Ref 4) and Wood and Sare (Ref 50) suggest that the contact resistance is large over a significant portion of the interfacial area. Experimental data from Moreau et al. (Ref 31) also suggest that the contact resistance varies significantly over the splat/substrate interface.

The existence of a contact resistance is much more important in thermal spray applications than in the millimeter-size droplet experiments (Fig. 4). The resistance to heat flow away from the solid/liquid interface includes two resistors in series: the transfer of heat across the solidified layer (of thickness δ) and across the contact resistance (\mathcal{R}). Equation 21 shows that the contact resistance is much more dominant in limiting the heat flux (Q) for smaller-size droplets (which would have smaller solidified thicknesses δ):

$$Q = \frac{T_{\text{melt}} - T_b}{R + \delta/K_S} \quad (\text{Eq 21})$$

Furthermore, the Madejski solidification theory fails to account for any time delay for nucleation of the solid phase due to undercooling of the liquid phase (Ref 1). Again, this phenomenon may be more important for the smaller particles where the thermal transient is orders of magnitude shorter in duration. Clyne (Ref 51) has shown that a 5 μm aluminum splat on a copper substrate can result in a delay of 6 ms before a significant (0.5 μm) solidified layer can form. This delay is due to the inclusion of both a contact resistance and undercooling in Clyne's model. As stated by Clyne, his result is of "dubious accuracy" but serves an "illustrative purpose." Lack of accurate property data prevents accurate prediction of rapid solidification rates. However, Clyne's nucleation delay is an order of magnitude longer than the impact time.

This suggests that an additional dimensionless number should be used to determine when contact resistances and nucleation delays are important. A number that is the ratio of the nucleation time to the impact time is proposed. The nucleation time can be estimated from the temperature change between the initial splat temperature to the nucleation temperature divided by the droplet cooling rate:

$$\Delta t_N = \frac{T_L - T_N}{\dot{T}} \quad (\text{Eq 22})$$

The nucleation temperature (T_N) can be calculated from the non-dimensional homogeneous solidification temperature (θ):

$$T_N = T_{\text{melt}} - \frac{\theta L}{C_L} \quad (\text{Eq 23})$$

Use of the homogeneous solidification temperature as the nucleation temperature should yield the maximum possible nucleation time delay. Clyne (Ref 51) estimated that θ is approximately 0.5 for metals. Thus, the ratio of the nucleation time to the impact time can be expressed as the following dimensionless number (assuming that the initial droplet temperature is near the melting temperature):

$$N = \frac{0.5Lu}{TC_L d} \quad (\text{Eq 24})$$

When N is small, delays in nucleation need not be considered. N is indeed small for the millimeter-size droplet experiments, but it is five orders of magnitude larger for thermal spray applications (which have smaller droplets at higher speeds). Therefore, extrapolation of the millimeter-size results to thermal spray applications is not justified.

Obtaining models for accurate predictions of contact resistances and rapid solidification parameters is difficult, and thus so too is numerical prediction of flattening ratios of thermal spray droplets. Experimentally derived parameter values need to be developed. However, the preceding discussion suggests that scaling of millimeter-size droplet results to thermal spray conditions is not possible.

5.3 Experimental Flattening Results for Thermal Spray Conditions

Relying only on experimental results at thermal spray conditions to determine flattening ratios is also difficult. Data for the flattening ratio taken under thermal spray conditions are sparse and display a large amount of scatter. Also, the techniques often used to measure initial droplet parameters are not very accurate. The following review of experimental data taken at thermal spray conditions will illustrate that the results are not conclusive.

In examining the Madejski plasma-sprayed alumina results, this author was unable to obtain the same nondimensional parameter values as Madejski. Madejski claimed that the left-hand side of Eq 20 was equal to 3.1 in his experiments. Using data for the heat of fusion of alumina ($1 \times 10^6 \text{ J/kg}$ [Ref 52]) and the heat capacitance of alumina ($1000 \text{ J/kg} \cdot ^\circ\text{C}$ [Ref 53]), this author calculated that the substrate had to be approximately 3100 K below the melting point of alumina (2318 K [Ref 52] or 2316 K [Ref 53]). This is not possible. Obviously, Madejski was using other property estimates in his analysis. Calculations using the property data given here (and assuming a reasonable substrate temperature) determined that the Madejski flow model resulted in a flattening ratio of 4.9 and the Madejski solidification model resulted in a flattening ratio of 4.6. Due to the similarity in the results, plasma-sprayed alumina cannot be used to distinguish between the two models. Experimentally, Madejski found a flattening ratio between 5 and 6, which is in agreement with both of the models.

Vardelle et al. (Ref 54) claimed that their results were in "excellent agreement" with the Madejski flow model. The conditions of these experiments are almost identical to the conditions of the Madejski thermal spray experiments reported in the preceding paragraph. Vardelle et al. claimed that the Madejski flow model results in a flattening ratio of about 4 for their average condition, which is in "excellent agreement" with their experimental result of 2.5 to 3.5. Again, the properties Vardelle et al. used must be slightly different, for this author predicted a flattening ratio of 4.9 using the Madejski flow model.

Plasma spray data from Fantassi et al. (Ref 5) were claimed to be in agreement with the Yoshida model. The Yoshida model is similar in form to Madejski's flow model:

$$\zeta = 0.83 \text{ Re}^{0.2} \quad (\text{Eq 25})$$

Equation 25 yields results 35% below the Madejski flow model (Eq 6). Fantassi et al. (Ref 5) presented detailed experimental conditions for a single data point. When the present author examined this case, flattening ratios of 5.0 with the Madejski flow model and 5.6 with the Madejski solidification model were obtained. This is the only thermal spray application **found** where the solidification model resulted in a larger flattening ratio than the flow model (due to the low thermal conductivity of the zirconia used in this experiment)—which compares poorly with the flattening ratio of 2 that was reported for this experiment. However, examination of the cumulative results shows that the flattening ratio found displayed considerable scatter, varying from 1.5 to 5.5 for conditions nominally similar to the experiment presented in detail. This high degree of variability is likely due to the inaccurate technique that was used to measure both droplet and splat size in this experiment.

Hasui et al. (Ref 25) present no flattening ratios, but do demonstrate that the coating properties and splat shapes are significantly altered by relatively modest changes in substrate temperature. Star-shaped patterns result when alumina droplets impact a cold substrate (300 K), and regularly shaped disks form when the droplets impact a heated surface (650 K). This result was verified by Sandia National Laboratories (Fig. 1). To determine whether the difference was due to an oxide coating created by heating of the steel substrate, Hasui et al. (Ref 25) observed splats on cold oxidized and cold polished steel substrates. These experiments resulted in identical star-shaped splats, which indicates that the surface finish was not a factor. It was therefore concluded that surface temperature and not surface finish, must influence the droplet flow after impact.

The two substrate temperatures examined by Hasui et al. (Ref 25) are both low compared to the molten temperature of alumina, and thus the cooling heat flux as modeled by Eq 21 would not significantly change. Therefore, if the solidification rate is to be influenced by the relatively small change in substrate temperature, the contact resistance or nucleation time delays must vary with substrate temperature.

Kudinov et al. (Ref 30) stated that star-shaped splats similar to those observed by Hasui et al. (Ref 25) result from higher droplet temperatures, higher droplet velocities, smaller droplet size, and reduced wetting. No mention was made of a colder substrate, which was found to be the controlling parameter by Hasui et al. (Ref 25), Savic and Boulton (Ref 16), and the data shown in Fig. 1. Moreau et al. (Ref 31) stated that splat shapes vary depending on the wettability of the substrate and that a combination that wets easily exhibits a lower thermal contact resistance. The faster cooldown due to the lower contact resistance in this experiment did not result in the star-shaped splats associated with colder substrates. The flow in the time period between the point when the splat is spread out to its maximum size and the end of solidification is dominated by surface tension forces. The variation in the length of this time period, and the variation in the surface-tension-induced movements (which vary with the contact angle), complicate comparisons between experiments.

Data from Moreau et al. (Ref 31) show that the solidification of plasma-sprayed molybdenum requires approximately 10 ms. This is in agreement with data from Fantassi et al. (Ref 5), which show that the solidification of plasma-sprayed zirconia also requires 10 ms. These times are orders-of-magnitude longer than the impact times. Moreau et al. (Ref 31) calculated contact resistances between plasma-sprayed molybdenum and various substrates (on the order of $1 \times 10^{-6} \text{ K} \cdot \text{m}^2/\text{W}$). This is in general agreement with what was assumed by Clyne (Ref 51) (1×10^{-4} to $1 \times 10^{-6} \text{ K} \cdot \text{m}^2/\text{W}$) and Jones (Ref 46) ($2 \times 10^{-5} \text{ K} \cdot \text{m}^2/\text{W}$), and what was measured by Fantassi et al. (Ref 5) ($2 \times 10^{-6} \text{ K} \cdot \text{m}^2/\text{W}$). Moreau et al. (Ref 31) showed that the contact resistance is lower as the coating builds, indicating that the molybdenum wets itself better than the various substrates used.

6. More Complex Models of Thermal Spray Droplet Impact

Numerical simulation of the impact and solidification process is presented by Solonenko (Ref 22) and Trapaga et al. (Ref

23). These models are compared to their own experimental data for millimeter-size droplet impacts. As mentioned earlier, scaling of these results to the plasma spray application of micron-size droplets is questionable. Trapaga et al. (Ref 23) showed that the existence of a contact resistance does not greatly influence final splat size. However, this conclusion is not likely to be valid for thermal spray applications.

Liu et al. (Ref 55) added the effects of solidification to their earlier reported isothermal impact calculations (Ref 39). Their model does not include contact resistance, and thus they conclude that the solidification process greatly limits the growth of the splat. The calculated splat diameters seem small and are not compared to experimental data. However, this paper provides a good starting point for modeling impact with solidification. As solidification models become more accurate, incorporating contact resistances and nucleation time delays, more accurate predictions of impact dynamics may be possible.

7. Conclusions

This review has determined that splashing has been largely ignored by studies of the impact of molten thermal spray droplets. However, experimental studies in other fields suggest that this process may be important. Droplet splashing affects deposition efficiency and may also affect the amount of oxides that are incorporated in the coating; the small splashed particles oxidize quickly and can be driven back onto the surface by the gas flow field associated with thermal spraying. Porosity and bond strength may also depend on the amount of splashing.

Splashing has received considerable attention in rain erosion studies. It has been found that splashing of a liquid (that does not change phase) will not occur during normal impact upon smooth, dry surfaces. As surface roughness increases, the amount of material that splashes increases. None of the studies presents a nondimensional roughness parameter that would allow extension of the rainwater results to thermal spray applications. There is some indication that if the liquid droplet undergoes a phase change during the impact process, splashing will occur even during normal impact on a smooth surface.

Studies of thermal spray particle impact generally have ignored the effect of solidification because scaling arguments and experimental evidence have indicated that the solidification time is typically two orders of magnitude longer than the flow time. However, experimental evidence has shown that colder substrates can significantly change the final splat shape from a disk to a star. It is unclear whether the star-shaped splats are a result of surface-tension-induced flows after the impact event is over, or whether they are caused by splashing. Work needs to focus on splashing during thermal spraying and to examine the effects of surface roughness and simultaneous solidification of the splat.

Millimeter-size droplet experiments do not scale easily to thermal spray conditions. Nucleation time delays become increasingly important as the physical size of the droplet decreases and the impact velocity increases. These time delays are caused both by contact resistances and undercooling of the droplet, factors which are often ignored in models of thermal spray droplet solidification.


Experimental observations of droplet impact under conditions typical of thermal spray applications are difficult due to the inability to accurately determine droplet size, velocity, and energy state just prior to impact. When flattening data are available, two other factors limit its usefulness in determining the proper scaling. First, high-temperature properties may not be available to reduce the data. Second, data using alumina are inconclusive, because the flow and solidification models proposed by Madejski yield similar results.

Acknowledgments

The author would like to acknowledge Raymond Cote for conducting the splat experiment presented in this paper and Barry Ritchey for the scanning electron microscopy work. This work was performed at Sandia National Laboratories and was supported by the U.S. Department of Energy under contract DEAC04-94AL85000.

References

1. D. Apelian, M. Paliwal, R.W. Smith, and W.F. Schilling, Melting and Solidification in Plasma Spray Deposition—Phenomenological Review, *Int. Met. Rev.*, Vol 28 (No. 5), 1983, p 271-294
2. Z.H. Zaat, A Quarter of a Century of Plasma Spraying, *Ann. Rev. Mater. Sci.*, Vol 13, 1983, p 9-42
3. I.A. Fisher, Variables Influencing the Characteristics of Plasma-Sprayed Coatings, *Int. Met. Rev.*, Vol 17, 1972, p 117-129
4. S. Safai and H. Herman, Plasma-Sprayed Materials, *Treat. Mater. Sci. Technol.*, Vol 20, 1981, p 183-214
5. S. Fantassi, M. Vardelle, A. Vardelle, and P. Fauchais, Influence of the Velocity of Plasma Sprayed Particles on the Splat Formation, *Thermal Spray Coatings: Research, Design and Applications*, C.C. Berndt and T.F. Bernecki, Ed., ASM International, 1993, p 1-6
6. D.R. Mash, N.E. Weare, and D.L. Walker, Process Variables in Plasma-Jet Spraying, *J. Met.*, Vol 13, 1961, p 473-478
7. S.E. Hinkle, Water Drop Kinetic Energy and Momentum Measurement Considerations, *Appl. Eng. Agric.*, Vol 5 (No. 3), 1979, p 386-391
8. C.D. Stow and R.D. Stainer, The Physical Products of a Splashing Water Drop, *J. Meteorolog. Soc. Jpn.*, Vol 55, 1977, p 518-532
9. Z. Levin and P.V. Hobbs, Splashing of Water Drops on Solid and Wetted Surfaces: Hydrodynamics and Charge Separation, *Philos. Trans. R. Soc. (London) A*, Vol 269, 1971, p 555-585
10. O.G. Engel, Waterdrop Collisions with Solid Surfaces, *J. Res. Nat. Bur. Stand.*, Vol 54 (No. 5), 1955, p 281-298
11. C.D. Stow and M.G. Hadfield, An Experimental Investigation of Fluid Flow Resulting from the Impact of a Water Drop with an Unyielding Dry Surface, *Proc. R. Soc. (London) A*, Vol 373, 1981, p 419-441
12. S. Chandra and C.T. Avedisian, On the Collision of a Droplet with a Solid Surface, *Proc. R. Soc. (London) A*, Vol 432, 1991, p 13-41
13. L. Cheng, Dynamic Spreading of Drops Impacting onto a Solid Surface, *Ind. Eng. Chem., Process Des. Dev.*, Vol 16 (No. 2), 1977, p 192-197
14. T.A. Elliott and D.M. Ford, Dynamic Contact Angles, *J. Chem. Soc. Faraday Trans.*, Vol 68, 1972, p 1814-1823
15. H.-H. Shi and J.P. Dear, Oblique High-Speed Liquid-Solid Impact, *JSME Int. J., Ser. I*, Vol 35 (No. 3), 1992, p 285-295
16. P. Savic and G.T. Boulton, The Fluid Flow Associated with the Impact of Liquid Drops with Solid Surfaces, *Proc. Heat Transfer Fluid Mech. Inst.*, 1957, p 43-84
17. J.L. Zable, Splatting during Ink Jet Printing, *IBM J. Res. Develop.*, Vol 21 (No. 4), 1977, p 315-320
18. Y. Wanibe, T. Itoh, and Y. Matsui, Impact Atomization of Liquid Metals, *Int. J. Powder Metall.*, Vol 27 (No. 3), 1991, p 195-209
19. M. Paliwal and R.J. Holland, Production of Fine Powders via Microatomization, *Adv. Powder Metall.*, Vol 3, 1989, p 35-44
20. D.T. Liles and D.C. Deleeuw, Rapid Solidification via Centrifugal Atomization with a Volatile Liquid Coolant, *Proc. TMS-AIME Northeast Regional Meeting on Rapidly Solidified Crystalline Alloys*, S.K. Das, B.H. Kear, and C.M. Adam, Ed., AIME, 1985, p 285-290
21. J. Madejski, Solidification of Droplets on a Cold Surface, *Int. J. Heat Mass Transfer*, Vol 19, 1976, p 1009-1013
22. O.P. Solonenko, The Fundamental Thermophysical Problems of Plasma-Spraying, *Thermal Spray: International Advances in Coatings Technology*, C.C. Berndt, Ed., ASM International, 1992, p 787-792
23. G. Trapaga, E.F. Matthys, J.J. Valencia, and J. Szekely, Fluid Flow, Heat Transfer, and Solidification of Molten Metal Droplets Impinging on Substrates: Comparison of Numerical and Experimental Results, *Metall. Trans. B*, Vol 23, 1992, p 701-718
24. D.G. Moore, A.G. Eubanks, H.R. Thornton, W.D. Hayes, Jr., and A.W. Crigler, "Studies of the Particle-Impact Process for Applying Ceramic and Cermet Coatings," AD-266381, National Bureau of Standards, Aug 1961
25. A. Hasui, S. Kitahara, and T. Fukushima, On Relation between Properties of Coating and Spraying Angle in Plasma Jet Spraying, *Trans. Natl. Res. Inst. Met.*, Vol 12 (No. 1), 1970, p 9-20
26. J.M. Houben, "Relation of the Adhesion of Plasma Sprayed Coatings to the Process Parameters Size, Velocity and Heat Content of the Spray Particles," Ph.D. thesis, Technische Universiteit Eindhoven, 1988
27. A.M. Worthington, *Study of Splashes*, Macmillan, 1963
28. M.F. Smith, R.A. Neiser, and R.C. Dykhuizen, "An Investigation of the Effects of Droplet Impact Angle in Thermal Spray Deposition," presented at the National Thermal Spray Conf. (Boston), 20-24 June 1994
29. P. Predecki, A.W. Mullendore, and N.J. Grant, A Study of the Splat Cooling Technique, *Trans. Metall. Soc. AIME*, Vol 233, 1965, p 1581-1586
30. V.V. Kudinov, P.Yu. Pekshev, and V.A. Safiullin, Forming of the Structure of Plasma-Sprayed Materials, *High-Temperature Dust Laden Jets*, O.P. Solonenko and Fedorchenko, Ed., VSP, NL, 1989, p 381-418
31. C. Moreau, M. Lamontagne, and P. Cielo, Influence of the Coating Thickness on the Cooling Rate of Plasma-Sprayed Particles Impinging on a Substrate, *Thermal Spray Coatings: Properties, Processes and Applications*, ASM International, 1992, p 237-243
32. X.L. Jiang, X.B. Fan, F. Gitzhofer, and M.F. Boulos, Induction Plasma Spraying of Refractory Materials, *Thermal Spray: International Advances in Coatings Technology*, C.C. Berndt, Ed., ASM International, 1992, p 39-44
33. O.P. Solonenko, M. Ushio, and A. Ohmori, Comprehensive Investigation of Metal Drop-Substrate Interaction, *Thermal Spray Coatings: Research, Design and Applications*, C.C. Berndt and T.F. Bernecki, Ed., ASM International, 1993, p 55-60
34. M.P. Planche, O. Betoule, J.F. Coudert, A. Grimaud, M. Vardelle, and P. Fauchais, Performance Characteristics of a Low Velocity Plasma Spray Torch, *Thermal Spray Coatings: Research, Design and Applications*, C.C. Berndt and T.F. Bernecki, Ed., ASM International, 1993, p 81-87
35. S. Fantassi, M. Vardelle, P. Fauchais, and C. Moreau, Investigation of the Splat Formation Versus Different Particulate Temperatures and Velocities Prior to Impact, *Thermal Spray: International Advances in Coatings Technology*, C.C. Berndt, Ed., ASM International, 1992, p 755-766
36. G. Trapaga and J. Szekely, Mathematical Modeling of the Isothermal Impingement of Liquid Droplets in Spraying Processes, *Metall. Trans. B*, Vol 22, 1991, p 901-914
37. F.H. Harlow and J.P. Shannon, The Splash of a Liquid Drop, *J. Appl. Phys.*, Vol 38 (No. 10), 1967, p 3855-3866

- 
38. T. Watanabe, I. Kuribayashi, T. Honda, and A. Kanzawa, Deformation and Solidification of a Droplet on a Cold Substrate, *Chem. Eng. Sci.*, Vol 47, 1992, p 3059-3065
 39. H. Liu, E.F. Lavernia, R.H. Rangel, E. Muehlberger, and A. Sickinger, Deformation and Interaction Behavior of Molten Droplets Impinging on a Flat Substrate in Plasma Spray Process, *Thermal Spray Coatings: Research, Design and Applications*, C.C. Berndt and T.F. Bernecki, Ed., ASM International, 1993, p 457-462
 40. F.J. Heymann, High-Speed Impact between a Liquid Drop and a Solid Surface, *J. Appl. Phys.*, Vol 40 (No. 13), 1969, p 5113-5122
 41. M.C. Rochester and J.H. Brunton, Pressure Distribution during Drop Impact, *Proc. 5th Int. Conf. Erosion by Solid and Liquid Impact*, J.E. Field, Ed., Cavendish Laboratory, Cambridge, U.K., 1979, p 6.1-6.7
 42. Y.C. Huang, F.G. Hammit, and W.-J. Yang, Hydrodynamic Phenomena during High-Speed Collision between Liquid Droplet and Rigid Plane, *J. Fluids Eng.*, 1973, p 276-294
 43. P.H. Pidsley, A Numerical Investigation of Water Drop Impact, *Proc. 6th Int. Conf. Erosion by Solid and Liquid Impact*, J.E. Field and N.S. Corney, Ed., Cavendish Laboratory, Cambridge, U.K., 1983, p 18.1-18.6
 44. M.B. Lesser and J.E. Field, The Geometric Wave Theory of Liquid Impact, *Proc. 6th Int. Conf. Erosion by Solid and Liquid Impact*, J.E. Field and N.S. Corney, Ed., Cavendish Laboratory, Cambridge, U.K., 1983, p 17.1-17.9
 45. J.E. Field, J.P. Dear, P.N.H. Davies, and M. Finnström, An Investigation of the Shock Structure and the Conditions for Jetting during Liquid Impact, *Proc. 6th Int. Conf. Erosion by Liquid and Solid Impact*, J.E. Field and N.S. Corney, Ed., Cavendish Laboratory, Cambridge, U.K., 1983, p 19.1-19.10
 46. H. Jones, Cooling, Freezing and Substrate Impact of Droplets Formed by Rotary Atomization, *J. Phys. D: Appl. Phys.*, Vol 4, 1971, p 1657-1660
 47. R. Fiedler and J. Naber, Estimating Film Size due to Drop Impact, *Proc. Combustion Institute Spring Technical Meeting on Combustion Fundamentals and Applications*, 1989, p 269-274
 48. E.B. Dussan V., On the Spreading of Liquids on Solid Surfaces: Static and Dynamic Contact Lines, *Ann. Rev. Fluid Mech.*, Vol 11, 1979, p 371-400
 49. H.S. Carslaw and J.C. Jaeger, *Conduction of Heat in Solids*, Clarendon Press, Oxford, 1984
 50. J. Wood and I. Sare, Experimental Observations of Crystal Growth in Alloys Rapidly Quenched from the Liquid State, *Metall. Trans. A*, Vol 6, 1975, p 2153-2155
 51. T.W. Clyne, Numerical Treatment of Rapid Solidification, *Metall. Trans. B*, Vol 15, 1984, p 369-381
 52. R.C. Weast, Ed., *CRC Handbook of Chemistry and Physics*, CRC Press, 1977
 53. Y.S. Touloukian, *Thermophysical Properties of High Temperature Solid Materials*, Vol 4, Macmillan, 1967
 54. A. Vardelle, M. Vardelle, R. McPherson, and P. Fauchais, Study of the Influence of Particle Temperature and Velocity Distribution within a Plasma Jet Coating Formation, *General Aspects of Thermal Spraying: 9th Int. Thermal Spraying Conf.*, J.H. Zaat, Ed., Netherlands Instituut voor Lastechniek, The Hague, 1980, p 155-161
 55. H. Liu, E.J. Lavernia, and R.H. Rangel, Numerical Simulation of Substrate Impact and Freezing of Droplets in Plasma Spray Processes, *J. Phys. D: Appl. Phys.*, Vol 26, 1993, p 1-9